DEVELOPING AND EXPLOITING A UNIQUE DATASET FROM SOUTH AFRICAN GOLD MINES FOR SOURCE CHARACTERIZATION AND WAVE PROPAGATION

Jordi Julià[1], Andrew A. Nyblade[1], Rengin Gök[2], William R. Walter[2], Lindsay Linzer[3], and Ray Durrheim[3]

Penn State University[1], Lawrence Livermore National Laboratory[2], and
Council for Scientific and Industrial Research[3]

Sponsored by the National Nuclear Security Administration

Award Nos. DE-FC52-06NA27320[1] and DE-AC52-07NA27344[2,3]
Proposal No. BAA06-06

ABSTRACT

In this project, we are developing and exploiting a unique seismic dataset to address the characteristics of small seismic events and the associated seismic signals observed at local (<200 km) and regional (<2000 km) distances. The dataset is being developed using mining-induced events from three deep gold mines in South Africa recorded on in-mine networks (<1 km) composed of tens of high-frequency sensors, a network of four broadband stations installed as part of this project at the surface around the mines (1–10 km), and a network of existing broadband seismic stations at local/regional distances (50–1000 km) from the mines. Data acquisition has now been completed and includes: (i) ~2 years (2007 and 2008) of continuous recording by the surface broadband array, and (ii) tens of thousands of mine tremors in the -3.4 < ML < 4.4 local magnitude range. Events with positive magnitudes are generally well recorded by the surface-mine stations, while magnitudes of 3.0 and larger are seen at regional distances (up to ~600 km) in high-pass filtered recordings.

We have now completed the quality control of the in-mine data gathered at the three gold mines included in this project. The quality control consisted of: (i) identification and analysis of outliers among the *P*- and *S*-wave travel-time picks reported by the in-mine network operator and (ii) verification of sensor orientations. The outliers have been identified through a 'Wadati filter' that searches for the largest subset of *P*- and *S*-wave travel-time picks consistent with a medium of uniform wave-speed. We have observed that outliers are generally picked at a few select stations. We have also detected that trigger times were mistakenly reported as origin times by the in-mine network operator, and corrections have been obtained from the intercept times in the Wadati diagrams. Sensor orientations have been verified through rotations into the local ray-coordinate system and, when possible, corrected by correlating waveforms obtained from theoretical and empirical rotation angles.

Full moment tensor solutions have been obtained for selected events within the Savuka network volume, with moment magnitudes in the 0.5 < Mw < 2.6 range. The solutions were obtained by inverting *P*-, *SV*-, and *SH*-spectral amplitudes measured on the theoretically rotated waveforms with visually assigned polarities. Most of the solutions have a non-zero implosive contribution (47 out of 76), while a small percentage is purely deviatoric (10 out of 76). The deviatoric moment tensors range from pure double couple to pure non-double couple mechanisms.

We have also calibrated the regional stations for seismic coda-derived source spectra and moment magnitude using the envelope methodology of Mayeda (2003). We tie the coda Mw to independent values from waveform modeling. The resulting coda-based source spectra of shallow mining-related events show significant spectral peaking that is not seen in deeper tectonic earthquakes. This coda peaking may be an independent method of identifying shallow events and is similar to coda peaking previously observed for Nevada explosions, where the frequency of the observed spectral peak correlates with the depth of burial (Murphy et al., 2009).

We are now investigating large magnitude events (ML > 3.0) in between the mines that were simultaneously recorded by the three in-mine networks and the surface-mine array. The purpose of this work is to determine joint hypocentral locations and full moment tensor solutions. One difficulty that we have encountered is that the timing systems are not synchronized among the mines. This difficulty can be circumvented when obtaining moment tensor solutions by inverting spectral amplitudes; however, relocating the seismic sources with the combined data set will require the introduction of network corrections in the equations. We expect the joint event locations and moment tensor solutions to be more robust than those obtained from individual in-mine or surface networks, and will allow the calibration of existing discrimination techniques at regional distances.

OBJECTIVES

The main objective of this project is to develop and exploit a unique seismic dataset from mine-related events recorded at in-mine (<3 km), local (3–10 km), and regional (>100 km) distances (Figure 1). The in-mine recordings are being obtained through three in-mine seismic networks consisting of a few tens of high-frequency geophones, which are routinely used to monitor seismic activity in the mines. The local recordings are being acquired through four broadband seismic stations (three Guralp CMG-3T and one Guralp CMG-40T feeding 24-bit RefTek data loggers) deployed under this project and located on the surface of the mining area. Additionally, the regional recordings are being acquired mostly through the AfricaArray stations in South Africa and surrounding countries. The dataset that we are assembling is unique in that it contains (1) events spanning several orders of magnitude, (2) events from a range of source depths, and (3) events from a variety of source types (e.g., pillar collapses, tensile fractures, normal and strike-slip faulting, and sources with a significant volumetric component).

We plan to exploit this dataset by using the mining events in 10 related areas of research aimed at improving U.S. operational capabilities to monitor for low-yield nuclear tests: (1) create an event catalog with accurate origin times and locations; (2) determine seismic moment, radiated energy, corner frequency, and stress drop; (3) obtain focal mechanisms from moment tensor inversion; (4) define several categories of event types (shear slip, tensile failure with volumetric component, explosions, pillar collapse) using focal mechanisms and in-mine observations; (5) define and calibrate a coda Mw scale for southern Africa; (6) using calibrated coda techniques, determine Mw for all cataloged events; (7) investigate the effects of depth and source mechanism on the coda-derived source spectra and evaluate the potential of using coda spectral peaking as a depth discriminant; (8) define and calibrate local-to-regional phase (direct *P* and *S*, *Pn*, *Pg*, *Sn* and *Lg*) propagation characteristics, including the use of the magnitude and distance amplitude corrections technique to determine appropriate geometrical spreading and frequency dependent Q values for the region; (9) characterize relative *P* and *S* excitation and source apparent stress resulting from variations in source parameters, including magnitude, mechanism, depth, rock characteristics, and source type; and (10) define regional phase ratios that can discriminate between the different source categories, and compare these discriminants and their performance with ongoing work done for other types of mining events, such as in Scandinavia and the western U.S.

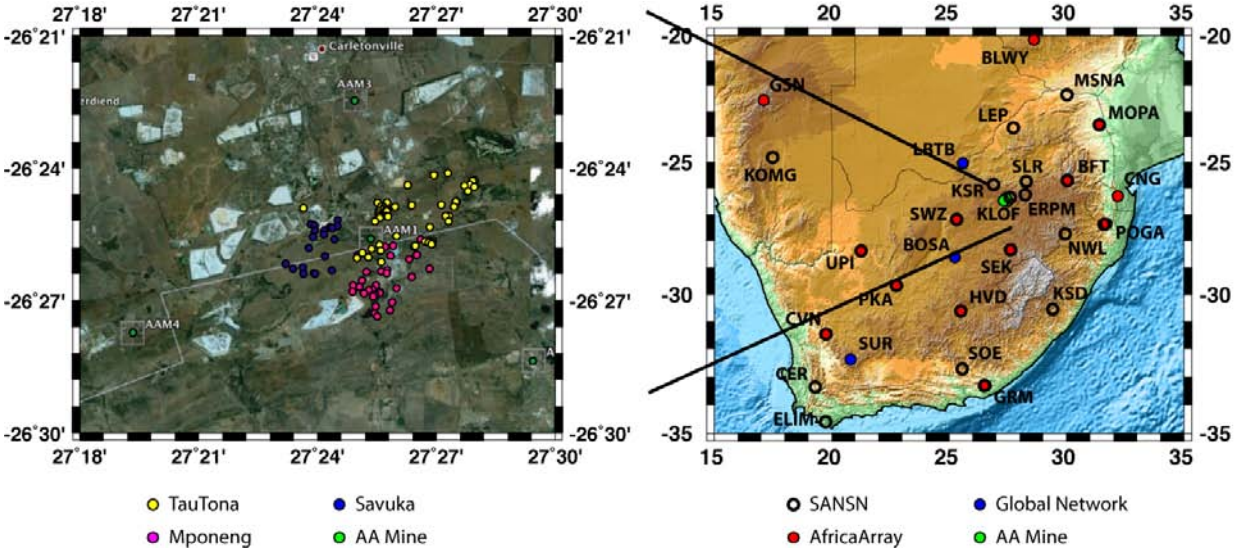

Figure 1. (left) Satellite image from Google Earth showing the Carletonville mining area where the three mines contributing to this project are located. The blue, magenta, and yellow dots are the surface projection of the Savuka, Mponeng, and TauTona in-mine networks, respectively, while the green dots are the surface broad-band stations deployed under this effort. (right) Map of broad-band stations in South Africa. The red dots are the AfricaArray stations, which are shared with the South Africa National Seismic Network (SANSN) shown as hollow circles, and the blue dots are the three permanent GSN stations.

RESEARCH ACCOMPLISHED

Data Gathering

The dataset acquired during this project includes proprietary waveforms for mine tremors recorded by three in-mine seismic networks in the Carletonville district of South Africa (Savuka, Mponeng, and TauTona) and continuous recordings of ground motion at four broadband seismic stations deployed at the surface around the mines (Figure 1).

The in-mine dataset is now complete and consists of high-frequency recordings for tens of thousands of mine tremors occuring during years 2007 and 2008. More specifically, the assembled data set consists of 22,317 events at Savuka with local magnitudes in the $-3.4 < ML < 4.5$ range, 38,915 events at Mponeng with magnitudes in the $-3.8 < ML < 4.7$ range, and 70,861 events at TauTona with magnitudes in the $-4.4 < ML < 4.9$ range, as catalogued by the in-mine network operator Integrated Seismic Systems International (ISSI). The in-mine networks are capable of recording tremors generated at nearby mines, so some overlap exists among the three catalogs.

The data have been provided to us in ASCII format and they have been converted to SAC in order to build the assembled data set. One difficulty when building the database has been identifying the number of stations in each network. The in-mine network operator (ISSI) does not use station names and simply attaches the location and instrument response information to the header of each data file. After counting and sorting all header information, we have identified 24 three-component, high-frequency geophones, with natural frequencies of 4.5, 14, and 28 Hz for Savuka; 80 three-component, high-frequency geophones, with natural frequencies of 4.5, 10, 14, 28, and 30 Hz for Mponeng; and 82 three-component, high-frequency geophones, with natural frequencies at 4.5, 10, 14, 28, and 30 Hz for TauTona. Station names have been given according to SAVXX, MPOXX, and TAUXX, where XX is a 2-digit code arbitrarily assigned to the site, for Savuka, Mponeng, and TauTona stations, respectively. In some instances, we observed up to three different instrument responses for the same location and, in such a situation, we have used three different station names for the same location (one per instrument response).

The first surface-mine broadband station (AAM1) was deployed in January 2007, and three more stations were deployed during the remainder of 2007, which have been operating continuously after installation. The stations are serviced periodically by our South African colleagues and also archived at Penn State. The data holdings at Penn State extend to February 24th, 2009, for AAM1, AAM2, and AAM3, and to August 15th, 2008, for AAM4.

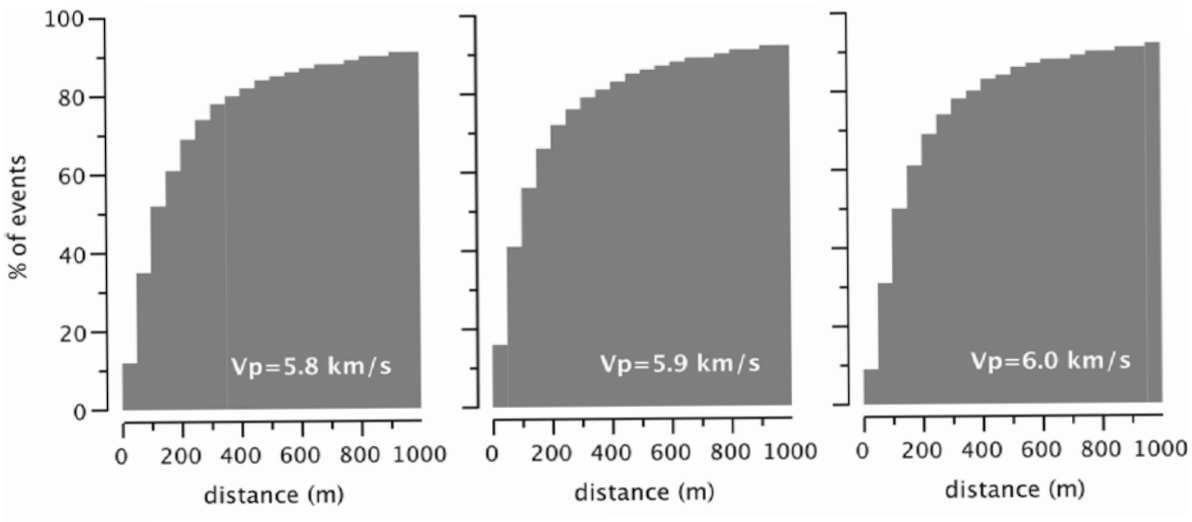

Figure 2. Cumulative histograms of hypocentral migration with respect to the original ISSI locations. The solutions closest to ISSI's are attained for a *P*-wave velocity of 5.9 km/s.

Event Catalogs

Event catalogs for 2007 and 2008 for each mine have been extracted from the header information stored in the original ASCII files. The catalog includes the origin time (South African local time), hypocentral location (in mine coordinates), and local magnitude as reported by ISSI. We have also built event catalogs reporting origin times in universal time (U.T.), locations in geodetic coordinates (lat and lon) and depths with respect to average mean sea level (AMSL).

During one of our visits to the ISSI branch in TauTona mine, we discovered that the origin times reported by ISSI are not actual origin times but trigger times used to label the events (more precisely, the trigger time corresponding to the first station recording a given event). Fortunately, ISSI included travel-time picks for *P* and *S* waves in the header information, and we have verified that accurate origin times can be recovered from the intercept time in Wadati diagrams (i.e., diagrams of *S-P vs P* travel time).

We have attempted a relocation of the seismic sources reported within the in-mine volume at Savuka in order to assess the robustness of the reported event locations. Travel-time picks for both *P* and *S* waves were included in the in-mine dataset, but not all the travel-time picks were utilized by ISSI to locate the seismic sources. To identify outliers we constructed Wadati diagrams from the reported travel-time picks and then utilized only travel-time picks falling along the corresponding Wadati lines in a simple Geiger inversion to relocate the events (see Julià et al., 2009a). Figure 2 displays the cumulative distribution of hypocentral migrations with respect to ISSI's original locations for assumed *P*-wave velocities of 5.8, 5.9, and 6.0 km/s. In all cases, more than 50% of the events migrate less than 150 m. Event locations are provided with an accuracy of ~50 m, according to ISSI.

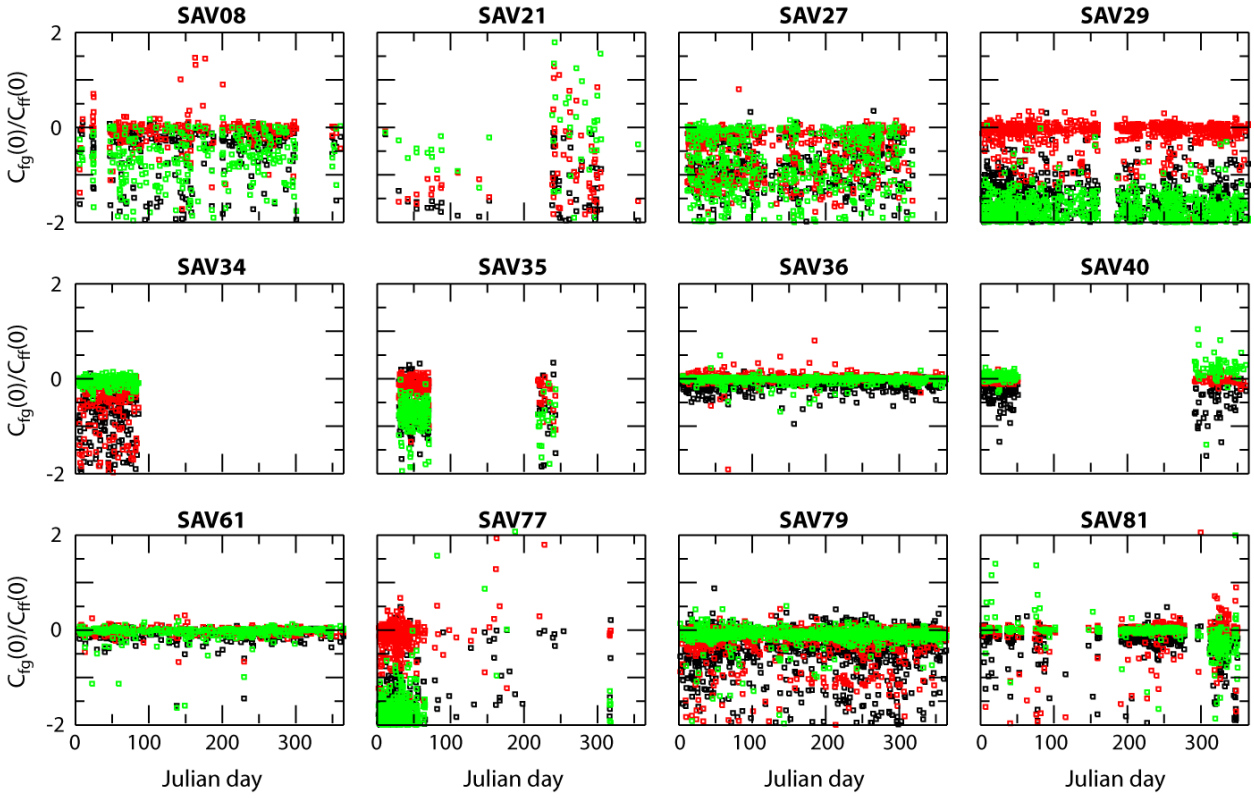

Figure 3. Correlation coefficients between theoretically and empirically rotated waveforms (green, SH; red, SV; black, P). Note that only stations SAV36, SAV40, SAV61, SAV79 and SAV81 show coefficients close to 1 in all three components.

Sensor Orientations

Sensor orientations have been verified for all three in-mine networks by comparing waveforms rotated into the local ray-coordinate system (P,SV,SH) through theoretical and empirical rotation angles. The theoretical angles were obtained from the station and event locations according to

$$\mathrm{tg}\ \varphi = (x_s - x_0)/(z_s - z_0) \quad (1)$$

$$\cos\phi = (z_s - z_0)/[(x_s - x_0)^2 + (z_s - z_0)^2]^{1/2}, \quad (2)$$

where x is North, y is East, and z is Up, and ϕ and φ are the take-off angle and azimuth, respectively, while the empirical rotation angles were obtained from the eigenvectors of the covariance matrix for the *P*-wavetrain as described in Montalbetti and Kanasewich (1970). By inspecting the correlation coefficients between the empirically and theoretically rotated waveforms we have been able to identify stations where both rotations disagree. Figure 3 illustrates the process for some stations operating during 2007 as part of the Savuka network. Note how stations SAV36, SAV40, SAV61, SAV79, and SAV81 have correlation coefficients close to one for all three components, demonstrating that the empirical and theoretical rotations agree. The remaining stations, on the other hand, show different patterns and suggest they have not been accurately oriented.

The procedure outlined above requires that the events be recorded in all three components. Unfortunately, some stations in the in-mine networks had at least one component failing during 2007 and 2008 and could not have the orientation verified. Overall, we found that empirical and theoretical rotations agree for 10 stations at Savuka (out of 19), 7 stations at Mponeng (out of 27), and 16 stations at TauTona (out of 32). Fortunately, we were able to work out corrections for some sensors by simply rotating the waveforms around the vertical axis, but uncertainties of 180^o might still exist due to the symmetry of the covariance matrix utilized for the empirical rotation.

Wadati Filter

We have devised a procedure based on Wadati diagrams to assess and improve the consistency of *P*- and *S*-wave travel-time picks with the assumption of propagation at constant wave-speed. The 'Wadati filter' is a simple search in the (*S*-*P*, *P*) travel-time space that finds the largest subset of (*S*-*P*, *P*) travel-time pairs that follow a straight line. Adjustable parameters include the minimum regression coefficient of the Wadati line, the minimum number of data points, and a range of slopes (which are closely related to the v_p/v_s ratio of the medium). The filter has been tested with travel-time picks reported by ISSI for events recorded by the Savuka in-mine network and we have found it quite effective in identifying defective travel-time picks, as well as travel-times associated to inhomogeneous ray-paths. An example is provided in Figure 4.

Moreover, by comparing histograms of *S*-*P* travel times with and without outliers for each station, we have observed that the majority of the outliers are picked at a reduced number of stations. Our interpretation is that most of the outliers are indeed travel-times associated to non-homogeneous ray-paths joining the event sources with a few select stations. These results are presently under review for publication in the South African Journal of Geology (Julià et al., 2009a).

Moment Tensor Solutions

We have obtained full moment tensor solutions for 76 events with moment magnitudes between 0.5 and 2.5 by inverting *P*, *SV*, and *SH* spectral amplitudes with polarity attached, as measured on mine tremors recorded by the Savuka in-mine network. We assumed a medium of uniform velocity and density (V_P=6.0 km/s, V_S=3.70 km/s, ρ=2.69 g/cm^3), so that the displacements could be expressed as (e.g., Udías, 2000):

$$u_i = G_{ij,k} m_{jk} \qquad i,j,k=1,2,3 \quad (3)$$

where

$$G_{ij,k} = (1/4\pi\rho v^3 R)\ \gamma_i\gamma_j\gamma_k\ \delta'(t-R/v) \qquad \gamma_i = x_i/R \quad (4)$$

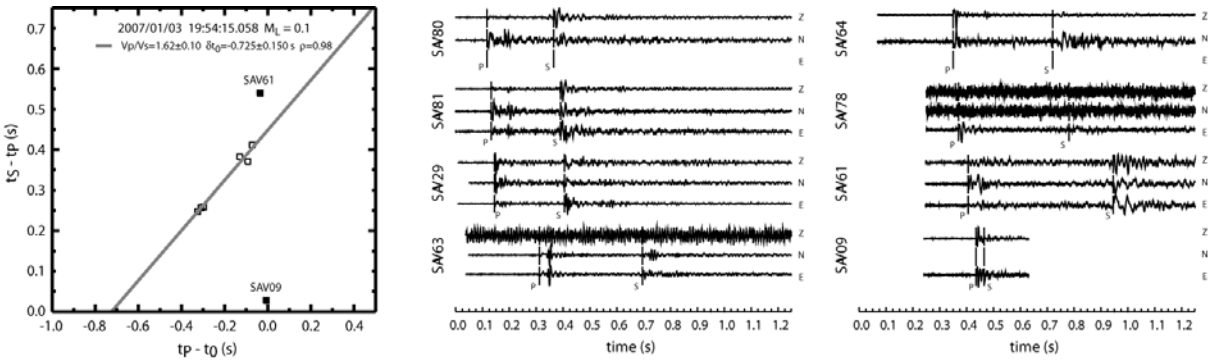

Figure 4. (left) Wadati diagram for a M_L = 0.4 event recorded at Savuka mine, South Africa. The solid squares are measurements rejected by the 'Wadati filter'. The time at the top is a trigger time randomly selected by ISSI to label the event, and used as a reference time in the diagram. (right) Recordings for the same events, sorted by *P*-wave travel-time. Note that the waveforms have been normalized to their maximum amplitude. Stations SAV80, SAV63, SAV64, SAV78, and SAV09 have failing channels.

and where ρ is density, v is the *P*- or *S*-wave velocity, and R is the hypocentral distance. The forward problem was then written by rotating the displacements into the ray-coordinate system and Fourier transforming the resulting equation to obtain spectral amplitudes. This defines a linear problem that was inverted by calculating the natural inverse through a singular value decomposition of the forward problem's matrix (e.g., Menke, 1989).

Spectral amplitudes from the in-mine recordings were obtained through the time-domain procedure of Urbancic et al. (1996). This procedure evaluates the spectral plateau of the *P*- or *S*-wave spectrum by computing the ratio

$$\Omega_o = 4(S_{D2})^{3/2}(S_{V2})^{-1/2} \quad (5)$$

where

$$S_{D2} = 2\int D^2(t)\,dt \quad S_{V2} = 2\int V^2(t)\,dt \quad (6)$$

and D(t) and V(t) are the displacement and velocity, respectively. Following Trifu et al. (2000), the integrals extend between the *P*- and *S*-wave travel times, for the *P*-wave amplitude, and twice the *S*-*P* time after the *S*-wave travel time for the SV and SH amplitudes. The polarity of the spectral amplitudes is assigned visually for each measurement by correlating low-pass filtered waveforms with synthetics.

Figure 5 displays the moment tensor inversion results for a Mw=1.6 event recorded by the Savuka in-mine network, along with the coverage of the focal sphere. The coverage of the focal sphere is limited, but characteristic of mining environments and reflecting the lack of station coverage ahead of the advancing mine stopes. However, the measured *P*- and *S*-wave amplitudes had both positive and negative polarities, which suggests that more than one energy lobe in the radiation pattern was sampled. The moment tensor solution obtained for this event is m_{xx}=-1.25x10^{11} Nm, m_{xy}=0.74x10^{11} Nm , m_{yy}=0.09x10^{11}Nm, m_{xz}=1.20x10^{11} Nm, m_{yz}=0.55x10^{11} Nm, and m_{zz}=-2.66x10^{11} Nm, and has a condition number around 0.16. The eigenvalues for this moment tensor solutions are σ_1=-3.35x10^{11} Nm, σ_2=-1.22x10^{11} Nm, and σ_3=0.74x10^{11} Nm, and $\mathbf{e}_1$ = (0.49,0.04,-0.87), $\mathbf{e}_2$ = (-0.72,0.57,-0.38), and $\mathbf{e}_3$ = (-0.49,-0.82,-0.31). The largest principal stress is thus compressive and oriented near-vertically (deflection from the vertical is ~29^o), consistent with gravity-driven stress conditions in a deep mine.

The trace for this particular moment tensor solution is tr(σ_i)= –3.83x10^{11} Nm, representative of an implosive volumetric source, and the deviatoric eigenvalues are σ^*_1 = -2.07x10^{11} Nm, σ^*_2 = 0.06x10^{11} Nm, and σ^*_3 = 2.01x10^{11} Nm, which are well approximated by a double-couple force equivalent. The eigenvectors of the deviatoric moment tensor are the same as those for the general moment tensor, so the double-couple solution thus has a sub-vertical pressure axis and a sub-horizontal tension axis characteristic of normal faulting. The decomposition of the moment tensor solution for this event thus indicates that stresses have been relaxed through normal faulting and co-seismic closure, consistent with previous findings in South African deep mines (McGarr, 1992a; 1992b).

The moment tensors for the 76 events recorded by the Savuka in-mine network are reported in Julià et al. (2009b) and can be found online at http://www.geosc.psu.edu/~jjulia/julia-esupp.html. The majority of the solutions reveal that the largest principal stress is vertical and compressive and that there is a significant implosive contribution, as illustrated in the example (Figure 5). The deviatoric components, on the other hand, can always be decomposed into two normal faults but other decompositions, such as combinations of DC and CLVD, are also possible.

Regional Coda Magnitudes and Spectra

We have also been looking at the seismic coda from regional events, both natural earthquakes and mine-related, that are recorded at regional stations across South Africa. Regional coda envelopes are useful to establish a calibrated moment magnitude scale for the area and to study source spectra of events.

We used the coda wave method of Mayeda (2003) to calculate source spectra of earthquakes recorded at GSN broad-band stations and the Kaapval seismic array. In order to generate a list of seismic events in the South Africa

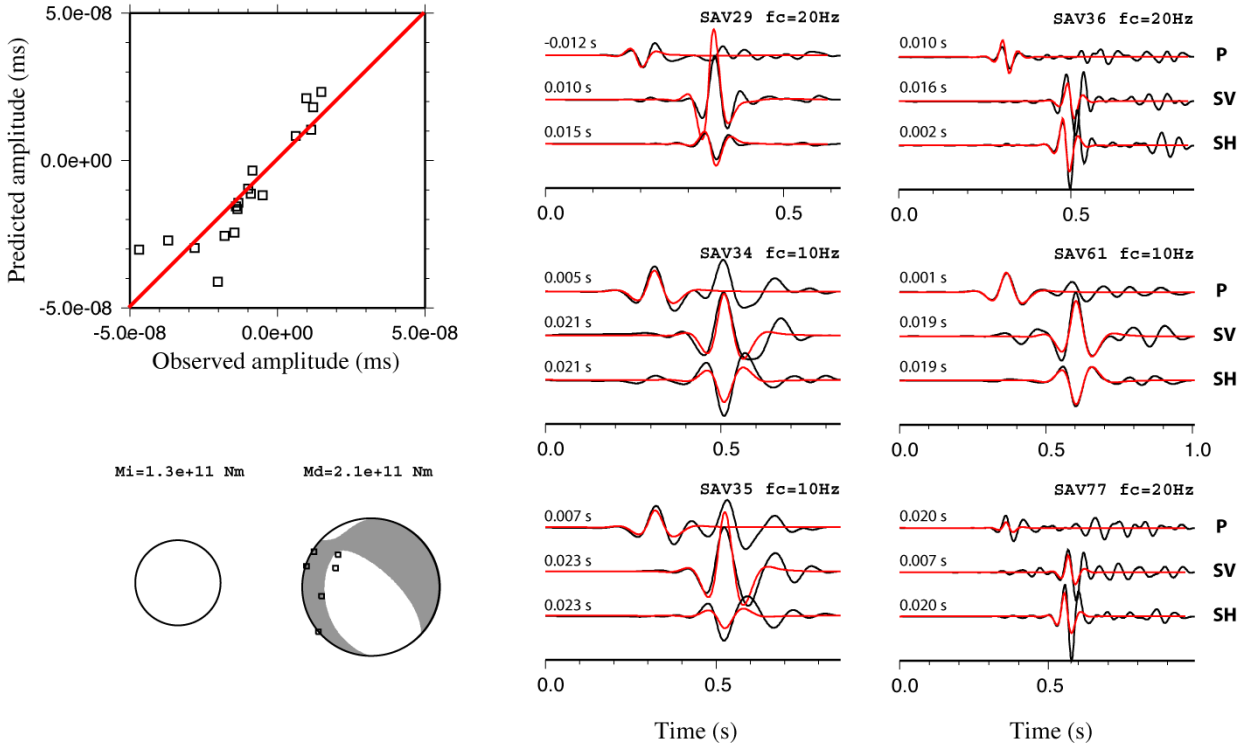

Figure 5. Moment tensor inversion results and coverage of the focal sphere for a ML=1.6 event recorded at Savuka mine. The upper left diagram compares predicted and observed spectral amplitudes for *P*, *SV*, and *SH* components. The lower left diagram shows the P-wave radiation pattern for the isotropic and deviatoric moment tensors, along with the coverage of the focal sphere (overlying the deviatoric "beach-ball"). The waveforms on the right are shown to compare the corresponding observed (black) and predicted (red) *P*, *SV* and *SH* amplitudes in the time domain. The event origin time is at t = 0 s and the synthetic waveforms have been shifted by the amount noted above each trace, to facilitate the comparison with the observations. The time shifts between observed and synthetic waveforms are due to inaccuracies in the event location, assumed wave-speed, and/or anisotropic effects. Note that only spectral amplitudes were inverted, so the observed time shifts did not influence our moment tensor solutions. The waveforms are shown in velocity.

mining districts, we used the seismic bulletins provided by the Council of Geoscience, Pretorai and the Preliminary Determination of Epicenters (PDE) catalogs. The mining-induced events were found to be concentrated around Welkom, Klerkdorp, (Far West, Central, and East) Rand regions. Tectonic events found in the bulletins primarily consisted of a large Mozambique (Mw=7.2) event and its aftershocks. The early and late coda parameters were obtained for a set of earthquakes in the region. Those parameters are distance dependent at each narrow frequency bands (0.05-6 Hz). The raw amplitudes were path corrected using the Street and Herrmann (ESH) method which corrects for geometrical spreading and Q. The path corrected amplitudes at 1.0-1.5 Hz are shown in Figure 1. To scale those non-dimensional amplitudes to absolute moment we use independently waveform modeled Mw's. A constant correction factor at each frequency band can then be used to correct for each event to obtain the moment rate function. We performed a grid-search procedure to obtain the body and surface wave fit at long-period levels. The best fitting is obtained at around 1-4 km and the mechanism is normal-type like. The shallow hypocentral location causes peaking of coda source spectra at 0.4-1.5 Hz. It is probably caused by strong excitation of Rayleigh waves at shallower depth that is then scattered into the coda (Figure 2). The spectral peaking causes overestimated Mw (coda)'s for smaller events where the long period coda levels cannot be measured. Larger magnitude mining induced events has the coda amplitude value up to 0.2-0.3 Hz narrow frequency band where we match the independently waveform modeled magnitudes. Whereas smaller magnitude events does not have an amplitude measurement at that frequency (Events 2 and 3, Figure 2). In other words, coda is abruptly eliminated below 0.2-0.3 Hz for smaller magnitude events. When we extrapolate that Mw value to the level we supposed measure from Table 2, we found that an average constant correction factor is 0.4-0.5.

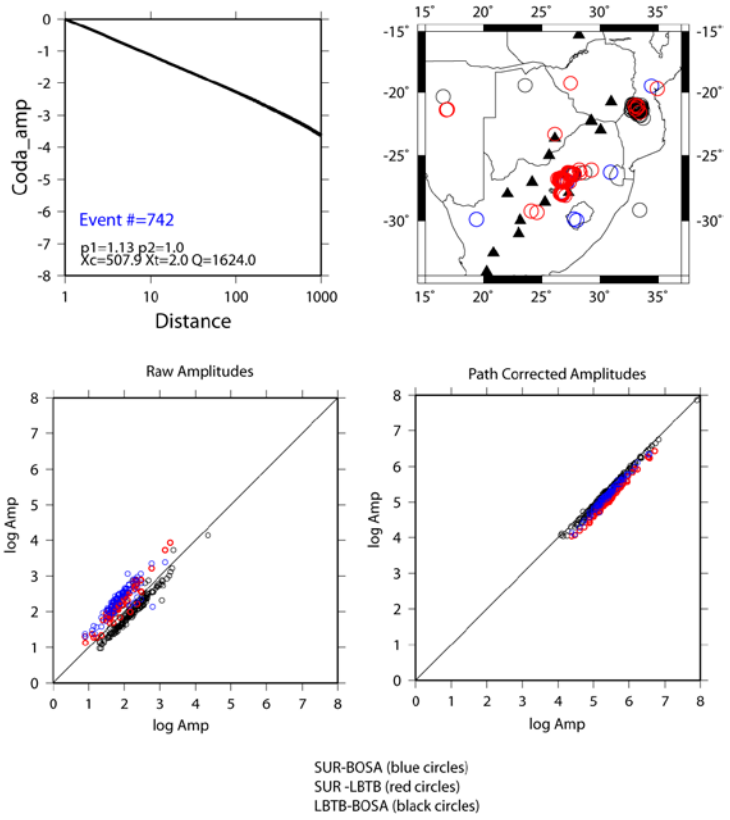

Figure 6. Path calibration at 1.0-1.5 Hz. Upper left panel is the ESH function.

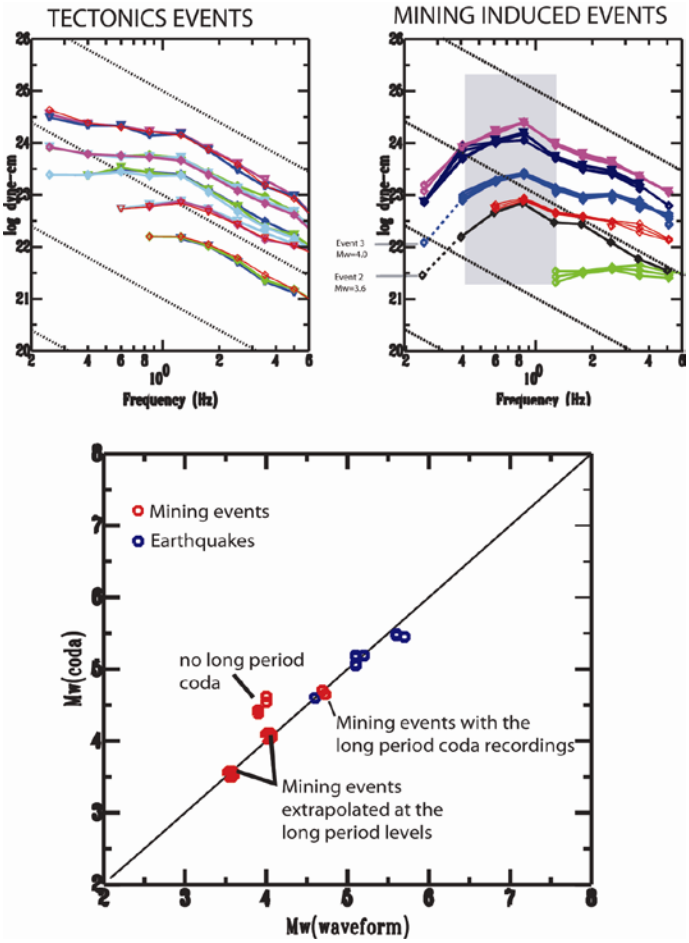

Figure 7. Coda derived source spectra from earthquakes (left) and mining induced events (right). The earthquakes have the usual shape: a near constant proportional to the moment at long periods and falling of as frequency^{-2} at the high frequencies. Coda based Mw's for any event can be determined from the long period level. In contrast the mine events show an unusual peaked shape, which may be an indicator of shallow depth due to Rg excitation and scattering into the coda. The lowest frequency points shown with dashed lines come from long period waveform modeling.

CONCLUSIONS AND RECOMMENDATIONS

So far, we have completed the quality control for all three in-mine networks and we have analyzed data recorded by the Savuka in-mine network only. For the moment tensor study (Julià et al., 2009b), we have used a subset of events with hypocenters located within the in-mine network volume and selected about 100 for which *P*, *SV*, and *SH* spectral amplitudes could be measured at 6 to 7 stations. The largest event included in this high-quality subset had a moment magnitude of 2.5, which was not large enough to be well recorded at regional distances.

We are now comparing the catalogs from the three in-mine networks to determine a subset of large (ML > 3.0) events with epicenters located within the combined networks, including the surface broadband array. Figure 8 shows a preliminary selection for the 2007 catalogs, which shows some large events are within the combined in-mine network. These events have an excellent azimuthal coverage, which will allow the determination of accurate event locations and moment tensor solutions. Discrepancies observed among the timing systems among the in-mine networks will be handled through network corrections and may introduce uncertainty in the event locations. Timing discrepancies, however, will seldom affect moment tensor solutions obtained from spectral amplitudes.

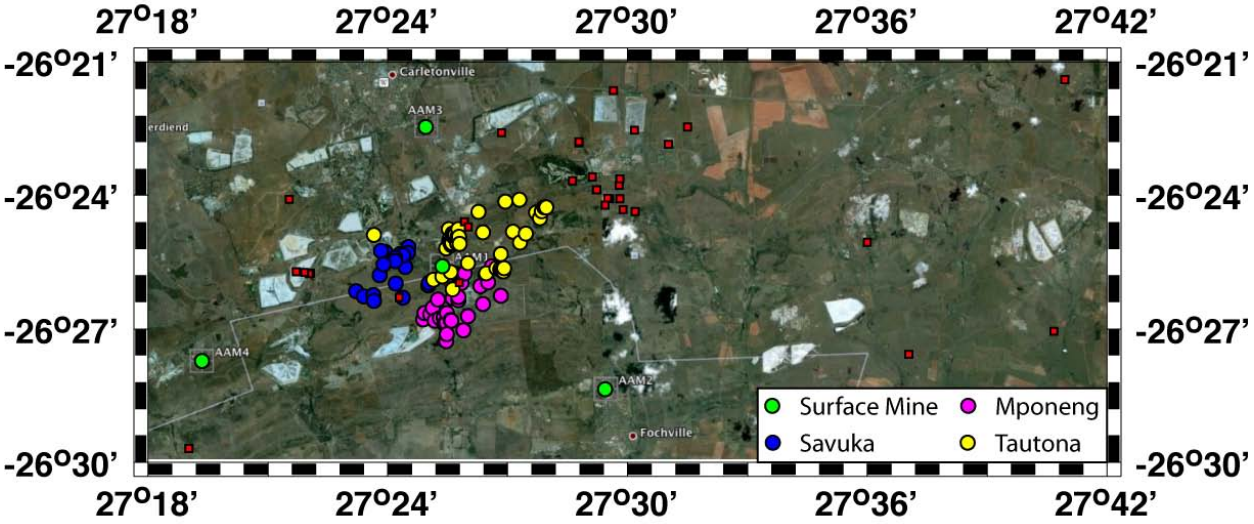

Figure 8. Events with magnitudes (ML) above 3.0 (red squares) recorded during 2007 at all three in-mine networks (color circles). A fair number of events are located within the combined network area. We expect to obtain robust locations and moment tensor solutions from the combined dataset.

ACKNOWLEDGEMENTS

We thank ISSI and Anglo Gold Ashanti for providing the seismic data and mine plans from the Savuka, Mponeng and TauTona mines. We also thank ISSI and the Council for Scientific and Industrial Research for assisting with event locations and solving other technical issues concerning the in-mine data, and we thank the Council for Geoscience for installing and operating the four broadband stations of the surface mine network. The IRIS data management center has provided assistance with archiving and distributing data from the permanent AfricaArray seismic stations, including data used in this study.

REFERENCES

Julià, J., A. A. Nyblade, R. J. Durrheim, L. Linzer, R. Gök, W. Walter, S. M. Spottiswoode, and P. Dirks (2009a). A Wadati filter for mine-induced seismicity, *S. Afr. J. Geol.*: in review.

Julià, J., A. A. Nyblade, R. J. Durrheim, L. Linzer, R. Gök, P. Dirks, and W. Walter (2009b). Source mechanisms of mine-related seismicity, Savuka mine, South Africa, *Bull. Seism. Soc. Am.*: in press.

Mayeda, K. (2003). Stable and transportable regional magnitudes based on coda-derived moment-rate spectra, *Bul. Seism. Soc. Am.* 93: 224–239.

Menke, W. (1989). *Geophysical Data Analysis: Discrete Inverse Theory*, Academic Press, 289 pp.

McGarr, A. (1992a). An implosive component in the seismic moment tensor of a mining-induced tremor, *Bull. Seism. Soc. Am.* 19: 1579–1582.

McGarr, A. (1992b). Moment tensors of ten Witwatersrand mine tremors, *Pure Appl. Geophys.*

Montalbetti, J. M., and E. R. Kanasewich (1970). Enhancement of teleseismic body waves with a polarization filter, *Geophys. J. R. Astr. Soc.* 21: 119–129.

Murphy, K. R., K. Mayeda, and W. R. Walter (2009). Lg-coda methods applied to Nevada Test Site events: Spectral peaking and yield estimation, *Bull. Seism. Soc. Am.* 99: 441–448.

Trifu, C. I., D. Angus, and V. Shumila (2000). A fast evaluation of the seismic moment tensor for induced seismicity, *Bull. Seism. Soc. Am* 90: 1521–1527.

Udías, A. (2000). *Principles of Seismology*, Cambridge University Press, 475 pp.

Urbancic, T.I., C.I. Trifu, R.A. Mercer, A.J. Feustel, and J.A.G. Alexander (1996). Automatic time-domain calculation of source parameters for the analysis of induced seismicity, *Bull. Seism. Soc. Am* 5: 1627–1633.